Journal of Oil Palm Research
DOI: https://doi.org/10.21894/jopr.2026.0032

A PLANT SPIRAL STUDY: AN AERIAL IMAGERY FOR FROND ANGLE MODELLING IN OIL PALM TREES

MUHAMMAD FITRI ABU MUNTALIB[1,3]*; MUHAMAD SAUFI MOHD KASSIM[1,2]; AIMRUN WAYAYOK[2]; AHMAD FIKRI ABDULLAH[2]; NUR 'ATIRAH MUHADI[2] and ZAILANI KHUZAIMAH[1]

ABSTRACT

Studying the plant spiral is essential for accurate frond number detection and canopy structure analysis. This study developed a two-dimensional phyllotaxis image template (2DPIT) for frond identification in oil palm trees. The template successfully identified the positions of frond number one (FN1), which serves as a reference point for determining the position of other fronds. Aerial data indicated that FN1 consistently exhibits the highest angular deviation, while frond number nine (FN9) showed minimal variation, confirming its near-vertical orientation. The deviation angles of FN1 and FN9 were analysed across various plantation ages using UAV-based and ground measurements. Overall, block differences were not significant, but interaction effects revealed age-related trends, with FN1 deviation peaking in older palms. A mathematical model was proposed to describe frond deviation as a function of frond number. Although a quadratic model was tested, an exponential decay model, proved to be more suitable, incorporating age-adjusted parameters for A and k. Model validation demonstrated strong performance, especially for right-handed spirals (Mean Absolute Error [MAE] = 3.02°, Root Mean Square Error [RMSE] = 3.85°), aligning with their dominance in oil palm phyllotaxis. These findings support the use of aerial imagery and spiral modelling as a non-destructive basis for future machine learning applications.

Keywords: canopy morphology, frond detection, oil palm, spiral phyllotaxis.

Received: 22 October 2025; **Accepted:** 4 June 2026; **Published online:** 11 August 2026.

INTRODUCTION

Oil palm currently stands as the most valuable crop industry, contributing significantly to Malaysia's economic sectors (Ahmad et al., 2024; Ali et al., 2024; Kushairi et al., 2019; Zachlod et al., 2025). The management of oil palm fronds (OPF) is essential for enhancing bunch productivity (Formaglio et al., 2021) and crop health monitoring (Amirruddin et al., 2020a). Conducting nutrient analysis of frond number 17 (FN17) is vital for assessing plant nutrient indicators (De Mello & Rozane, 2020; Janani & Jebakumar, 2022; Lundegårdh, 1943). Foliar traits, such as leaf dry matter content (LDMC) and specific leaf area (SLA), are well-recognised as important indicators of soil fertility (Daou et al., 2021). In the context of oil palm, these traits are particularly crucial, as the fronds serve as the primary unit for evaluating physiological status, nutrient allocation, and overall canopy health. However, the effectiveness of LDMC and SLA in predicting soil nutrient conditions remains a topic of ongoing debate, with some studies suggesting that LDMC may offer stronger explanatory power (Hodgson et al., 2011). Therefore, it is important to clearly identify and justify the number of fronds, especially the standard

[1] Institute of Plantation Studies (IKP), Universiti Putra Malaysia, 43400 UPM Serdang, Selangor, Malaysia.

[2] Department of Biological and Agricultural Engineering, Faculty of Engineering, Universiti Putra Malaysia, 43400 UPM Serdang, Selangor, Malaysia.

[3] Putra Agriculture Center, Universiti Putra Malaysia, 43400 UPM Serdang, Selangor, Malaysia.

* *Corresponding author e-mail: m_fitri@upm.edu.my*

reference fronds used for physiological and nutritional evaluations. This ensures that oil palm research and field tests are consistent, reliable and comparable.

Study on oil palm canopy morphology employs advanced sensing and modelling techniques to monitor health, optimise yields, and assess environmental impacts. Terrestrial laser scanning (TLS) and unmanned aerial vehicles (UAVs) have been used for conducting detailed canopy analyses. Furthermore, nutrient management and genetic selection have been shown to influence canopy structure and functionality (Azuan et al., 2019; Husin et al., 2020; Montoya-Sánchez et al., 2024). By integrating these methodologies, we can effectively promote sustainable plantation management and ecological monitoring.

Fronds numbers 1 (FN1), 9 (FN9) and 17 (FN17) are of significant importance in oil palm studies as they correspond to key developmental stages, facilitating accurate, standardised assessments of plant health, nutrient status and disease. Although FN1 is less frequently utilised for nutrient analysis, it plays a crucial role in detecting the earliest physiological responses (Khairunniza-Bejo et al., 2015). The FN9 is often preferred over the FN17 for the early detection of chlorophyll and nutrient status, particularly when employing remote sensing and machine learning techniques (Ahmadi et al., 2017; Amirruddin et al., 2020b;). In contrast, FN17 remains the industry standard for laboratory nutrient analysis in mature palms due to its sensitivity and reliability for nitrogen (N), phosphorus (P) and potassium (K) (Hariadi et al., 2024a; Kok et al., 2021; Tarmizi et al., 2017).

The current practice for frond determination in the field varies among farmers and is typically conducted by qualified individuals (Ahmad et al., 2025). Inaccurate detection of the FN1 position can result in erroneous identification of frond numbers. Destructive methods, such as selectively cutting leaflet areas on FN17 for nutritive analysis, are essential in oil palm management (Amirruddin et al., 2020a). Validating the efficiency of fertiliser uptake by the tree is important. Accurate detection and selection of fronds are crucial in oil palm management, as frond morphology and phenotyping can reliably indicate plant health status (Herman et al., 2024). Additionally, selective environmental pressures and phylogenetic constraints highlight the complex interplay between external conditions and the inherent characteristics of plants that influence leaf shape formation (Givnish, 1987). Consequently, errors in frond identification can lead to misinterpretation of crucial agronomic data, ultimately undermining decision-making processes related to crop productivity and the long-term sustainability of the plantation.

The use of UAVs in the plantation sector has become increasingly widespread (Khuzaimah et al., 2022). Aerial imaging systems are now widely used in oil palm plantation management systems, particularly for plant health monitoring (Ahmadi et al., 2022; Kouadio et al., 2023; Zheng et al., 2021). This approach enables faster, more efficient processing than traditional methods. FN1 serves as a key reference for detecting FN9 and FN17. Recent technological advancements have enabled the use of remote sensing tools for non-destructive frond analysis (Hariadi et al., 2024b). The non-destructive leaflet and frond analysis technique has proven to be more effective for identifying oil palm diseases (Ali et al., 2019). In studying the non-destructive method of nutritive measurement, accurately identifying the position of the oil palm fronds within their spiral arrangement is essential.

The arrangement of oil palm fronds, or phyllotaxis, follows the Fibonacci sequence and incorporates the golden ratio in the emergence of fronds and petals on the tree's shoot (Sah et al., 2020). In studies analysing oil palm leaflets, FN17 has been identified as a key reference point for assessing tree nutrition (Hariadi et al., 2024b; Jayaselan et al., 2017; Mohd Jefri et al., 2023). Observations indicate that FN17 is positioned slightly in alignment with both FN9 and the emergence of FN1. The right-handed spiral occurs when the frond arrangement follows a clockwise direction, while the left-handed spiral occurs in the opposite direction. Okabe et al. (2015) illustrate that the oil palm tree exhibits a golden angle derived from Fibonacci numbers, showing a divergence of 137.5° between one frond and subsequent fronds. There are two types of spiral rotation observed in the oil palm tree (Corley & Tinker, 2015), and these angles and spirals reflect the overall arrangement of fronds on the tree. However, accurately determining the frond number can be challenging for humans (Liu et al., 2022) and often leads to misjudgement about the type of spiral during field assessments (Li et al., 2018). To establish the number of fronds on an oil palm, it is essential to first detect the phyllotactic spiral rotation.

This study investigates the application of spiral phyllotaxis theory and aerial imagery for the non-destructive modelling of frond angles in oil palm. Its primary objective is to improve the identification of structurally significant fronds by developing and implementing a two-dimensional phyllotaxis image template (2DPIT). This template is based on the golden angle (137.5°), a fundamental principle of spiral phyllotaxis derived from the Fibonacci sequence. It is designed to simulate the natural divergence pattern of fronds within the canopy. By projecting sequential frond positions using uniform angular increments, this 2DPIT enables the alignment of observed aerial canopy data with theoretical spiral patterns.

The ultimate objective of this study is to develop a reliable, non-destructive method for determining the number of oil palm fronds by integrating geometric modelling with UAV-based image analysis. By statistically validating the predicted and measured frond divergence angles across tree ages and spiral orientations, this approach seeks to enhance the accuracy of frond position identification. Such advancement will enable more precise canopy assessments and enhance future applications in spectral sampling, nutrient monitoring and the precision management of oil palm plantations.

MATERIALS AND METHODS

In this study, the maturity stage of oil palm crowns was identified as a crucial phenological indicator of vegetative development. The oil palm crown reaches its maximum architectural development approximately 10 year after planting, marking the transition from the juvenile to mature growth phases (Corley & Tinker, 2015). Canopy development is closely related to light interception, photosynthetic efficiency, and the production of fresh fruit bunch (FFB). Crown expansion occurs between the 7th and 10th years post-planting under optimal agronomic conditions (Breure, 1985; Woittiez et al., 2017). The peak yield potential for FFB and oil palm growth is typically observed between 8 and 10 years after planting (Suhartono et al., 2023). Therefore, the selection of sampling palms during this critical growth phase was intentionally guided by existing study to ensure that the data collected accurately reflects the physiological and structural dynamics of crown development during its peak productivity phase.

Study Area

This study was conducted at an oil palm area located at Universiti Putra Malaysia in Serdang, Selangor, Malaysia (2°58′48′′ N and 101°43′48′′ E). A total of 300 oil palm samples were randomly selected from five distinct blocks within the UPM plantation. The ages of these blocks are as follows: Block A (13 years), Block B (12 years), Block C (15 years), Block D (18 years), and Block E (8 years). The samples were monitored at 14-day intervals throughout a six-month period. This sample size is consistent with previous studies that have effectively utilised sample sizes ranging from 100 to over 1,700 trees for analysing frond orientation and canopy structure in oil palm (Asyraf et al., 2022; Khairy & Syafi'i, 2025). Across all blocks, the average environmental conditions were at temperature of 29°C and humidity level of 73.1%. Additionally, the average rainfall was measured at 7.4 mm/day, with a recorded wind speed of 3.356 mph during image acquisition. The study area featured varying topographical conditions, with elevations ranging from 35–106 m above sea level for each sampling block. Image acquisition was performed at different altitudes, with consistent altitude measurements taken throughout the study.

Ground Data Collection

Spiral identification on the trunk. The study observed a frond spiral arrangement on oil palm trees. A pseudo-bark pattern was noted along the trunk, positioned upward toward the right or left when viewed from the side of the tree. The layers of pseudo-bark ascend to the left, indicating that this tree exhibits a left-handed spiral pattern. This spiral arrangement is essential for the template application in subsequent frond counting analysis (*Figure 1*).

Figure 2 illustrates how the trunk diameter was measured at breast height (1.3 m from above ground level), using linear reference markers projected onto the front-facing surface of the trunk. A horizontal white line spans the visible width of the trunk, representing the apparent diameter. To determine the actual trunk diameter, measurements were taken manually in the field with a measuring tape, allowing for the calibration of a scale factor derived from the image. The accuracy of this measurement was improved by ensuring that the image plane was perpendicular to the trunk axis, thus minimising parallax distortion.

The angular orientation of the fronds was determined by tracing angle vectors that originate from the centre of the trunk. The coloured lines blue, yellow and red represent the previous FN1, FN9 and FN17, respectively. To assess angular deviation, the angle between the blue central axis (designated as previous FN1), the yellow line (previous FN9) and the red line (previous FN17) was measured. These angles reflect the phyllotactic divergence of frond positions. AutoCAD's built-in angular measurement functions were used to extract precise angular values in degrees from one to another.

Stump cross-section analysis. A single oil palm tree was utilised for a stump cross-section analysis to examine the principle of Fibonacci. This study focused on measuring the divergence angles between the existing stump patterns. The stump will eventually develop into an oil palm frond. The Fibonacci principles, particularly the golden angle (137.5°), are employed in contemporary study on phyllotaxis and canopy pattern (Wang et al., 2022).

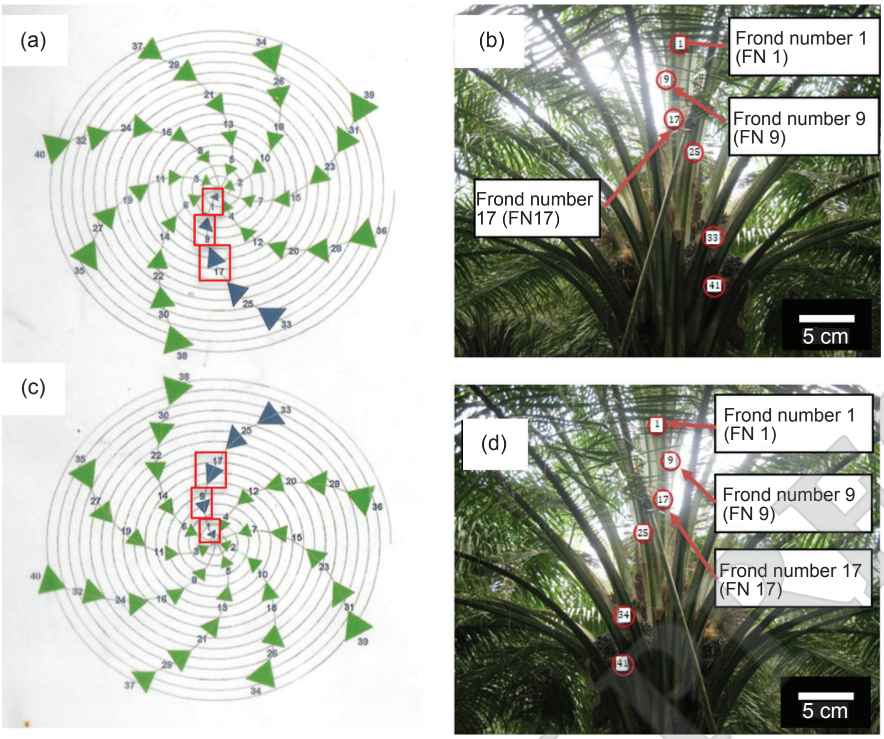

Figure 1. (a) Phyllotaxis in right-handed spiral from top-view, (b) right-handed spiral frond number 1, 9 and 17 from ground-view images, (c) phyllotaxis in left-handed spiral from top-view and (d) left-handed spiral frond number 1, 9, and 17 from ground-view images.

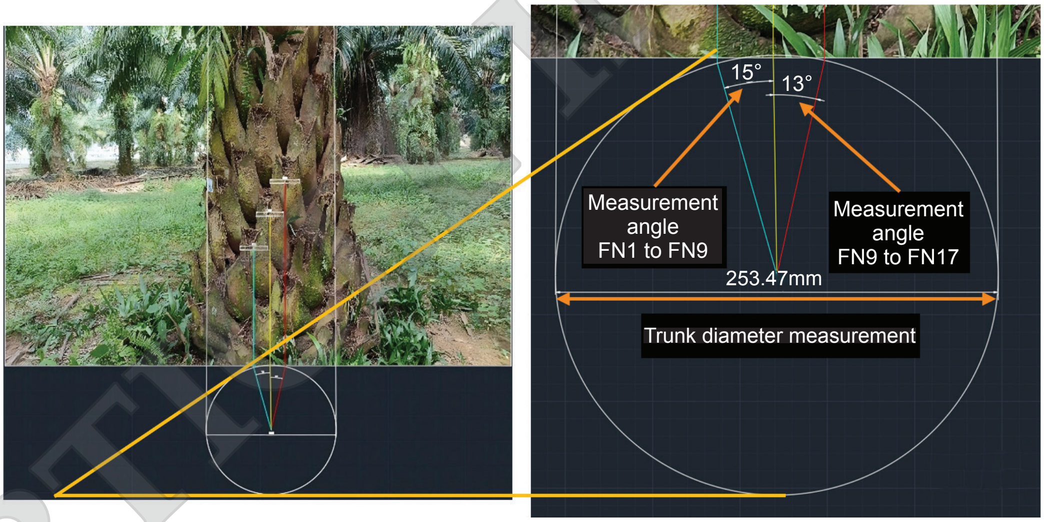

Note: Blue line - frond number 1 (FN1); Yellow line - front number 9 (FN9); Red line - front number 17 (FN17).

Figure 2. Geometric-based trunk and phyllotactic angle measurement using visual trunk projection corresponding to 1.3 m above ground level.

The crown cross-section analysis was conducted by felling a single palm tree, followed by tracing the phyllotactic pattern on tracing paper and scanning it for digital analysis (*Figure 3*). The variation in divergence angles was measured with angular tools in AutoCAD. This analysis aimed to verify the accuracy of the golden angle in the crown cross-section of an oil palm tree.

The stump cross-section analysis presented in this study is based on a single oil palm tree and is included solely for illustrative purposes. Specifically, it provides a direct geometric observation of the divergence angle, which approximates the theoretical golden angle (~137.5°) associated with Fibonacci phyllotaxis. This analysis is not used for statistical inference, model calibration or parameter estimation. All structural modelling and quantitative analyses in this study are derived from the UAV-based dataset comprising approximately 300 oil palm trees. The single-tree observation is intended only to support the conceptual interpretation of the spiral arrangement.

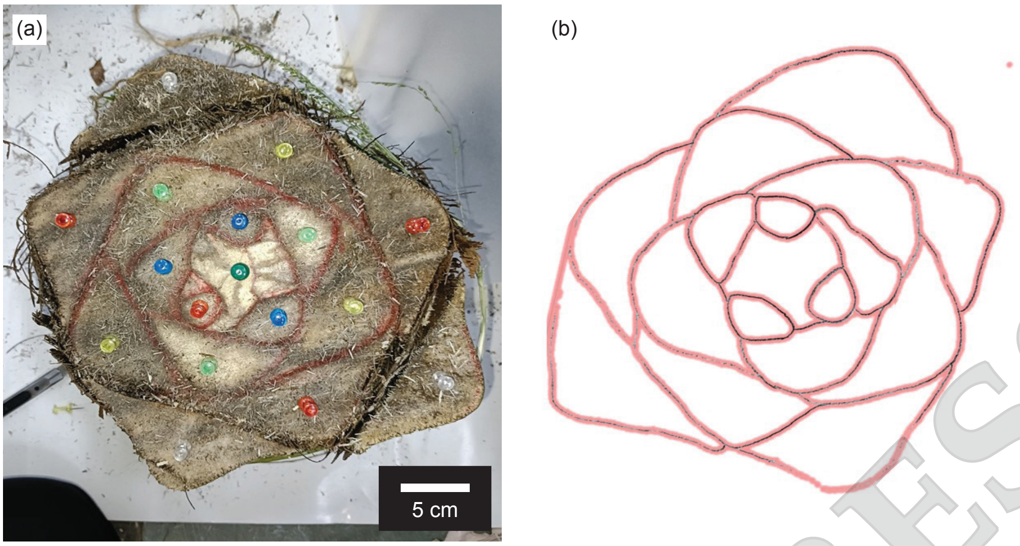

Figure 3. *(a) Estimation of the centre for angle measurement and (b) traced image to be processed in MATLAB to determine the centre of the object.*

Development of Two-Dimensional Phyllotaxis Image Template (2DPIT)

The 2DPIT was developed based on the Fibonacci angle sequence and the study conducted by Guzmán et al. (2022). This template illustrates the sequence of new frond emergence, occurring at an angle of 137.5° from the previous frond in relation to the apex centre. When the new frond (n) emerges, the total number of fronds increases by one ($n + 1$). The template was created using Microsoft PowerPoint 2023, which provides essential angle measurements and is user-friendly. Using this software, nine lines were drawn radiating from a common centre, each maintaining a diverging angle of 137.5° according to the sequence numbers. Two-line rotation arrangements were designed to represent left-handed or right-handed spiral arrangements. The final template was then overlaid with an aerial image of the oil palm canopy for further measurement using AutoCAD to determine the angle deviation of FN1 and FN9.

Data Acquisition

Equipment specification. An UAV, specifically the DJI Matrice 300 RTK (SZ DJI Technology Co., Ltd., China), was employed to capture aerial top views of the oil palm canopy. The DJI Matrice 300 RTK is an enterprise-grade UAV designed for industrial and research applications, featuring an impressive flight time of up to 55 min and a maximum payload capacity of 2.7 kg. Its advanced real-time kinematic (RTK) positioning capabilities facilitate high-accuracy mapping, making it exceptionally valuable for our project.

For this study, a multi-camera MicaSense RedEdge MX camera (MicaSense, Inc., USA) was mounted on a UAV. A flight altitude of 60 m above sea level (ASL) was chosen to accommodate the diverse topographical conditions of the study area, which ranges from 35–106 m ASL. Image acquisition was conducted at varying elevations, maintaining the same altitude as recommended in prior study, including the findings by Avtar et al. (2020), who suggested this altitude for effective monitoring of oil palm health. The imaging process followed a single flight path from south to north, optimising coverage while minimising shadow interference by conducting flights during cloud-free conditions between 10.00 am and 2.00 pm local time. The ground sample distance (GSD) for all images was set at 2.36 cm/pixel, ensuring a high level of detail and clarity in the captured visual data. This resolution enables precise analysis and interpretation of the imagery, making it suitable for a variety of applications.

To ensure reliable photogrammetric reconstruction, we maintained front and side overlaps of 80% and 70%, respectively, following the methodology outlined by Wong et al. (2023). Flight paths were carefully generated using automated mission planning software, which facilitated consistent coverage across the target areas. This approach enhances our capabilities in precision agriculture, canopy analysis and environmental monitoring, providing high-quality spectral data and precise georeferencing essential for effective analysis. For each ground-truth tree, the coordinates of the trunk centre were marked and FN1 was identified manually by an expert agronomist. Frond azimuth angles were measured using a digital compass and compared with the canopy orientation observed in UAV imagery. These measurements provided crucial reference data for assessing the accuracy of frond aerial detection.

Image preprocessing. A series of overlapping aerial images was processed using Agisoft Metashape Professional Version 2.2.0 (Agisoft LLC, Russia) to generate a georeferenced orthomosaic in geographic tagged image file format (GeoTIFF). We imported raw multispectral images captured by the MicaSense RedEdge-MX camera, configured as a multi-camera system, and included ground control points (GCPs) from a comma-separated values (CSV) file to improve georeferencing accuracy. High-precision photo alignment was achieved through a combination of generic and reference preselection methods, utilising carefully adjusted parameters for key and tie points.

Unmanned Aerial Vehicles (UAVs) Imaging Analysis

New frond production (FN1) for oil palms emerges in the frond spiral within 7–14 days (Guzmán et al., 2022; Prusinkiewicz et al., 2022). Based on this timeframe, UAV image acquisition was conducted consistently at 14-day intervals over a 6-month period to capture an aerial image of the oil palm crown.

Aerial image tree centre detection. To improve the accuracy of identifying the centre of the oil palm tree image, two divergent angles derived from the template were utilised. Identifying the centre can be challenging due to the ongoing debate surrounding the FN1 angles. As an alternative approach, the reverse measurement angle from frond number three (FN3) to frond number two (FN2) (indicated by the blue arrow in *Figure 4a*), and the forward diverging angle from FN2 to FN1 (indicated by the red arrow in *Figure 4b*) were employed. This angle confirms that the frond is fully open and positioned correctly. These angular relationships help in triangulating the true centre point of the phyllotaxis pattern. As shown in *Figure 4c*, both angles effectively align the template, confirming the detection of the centre.

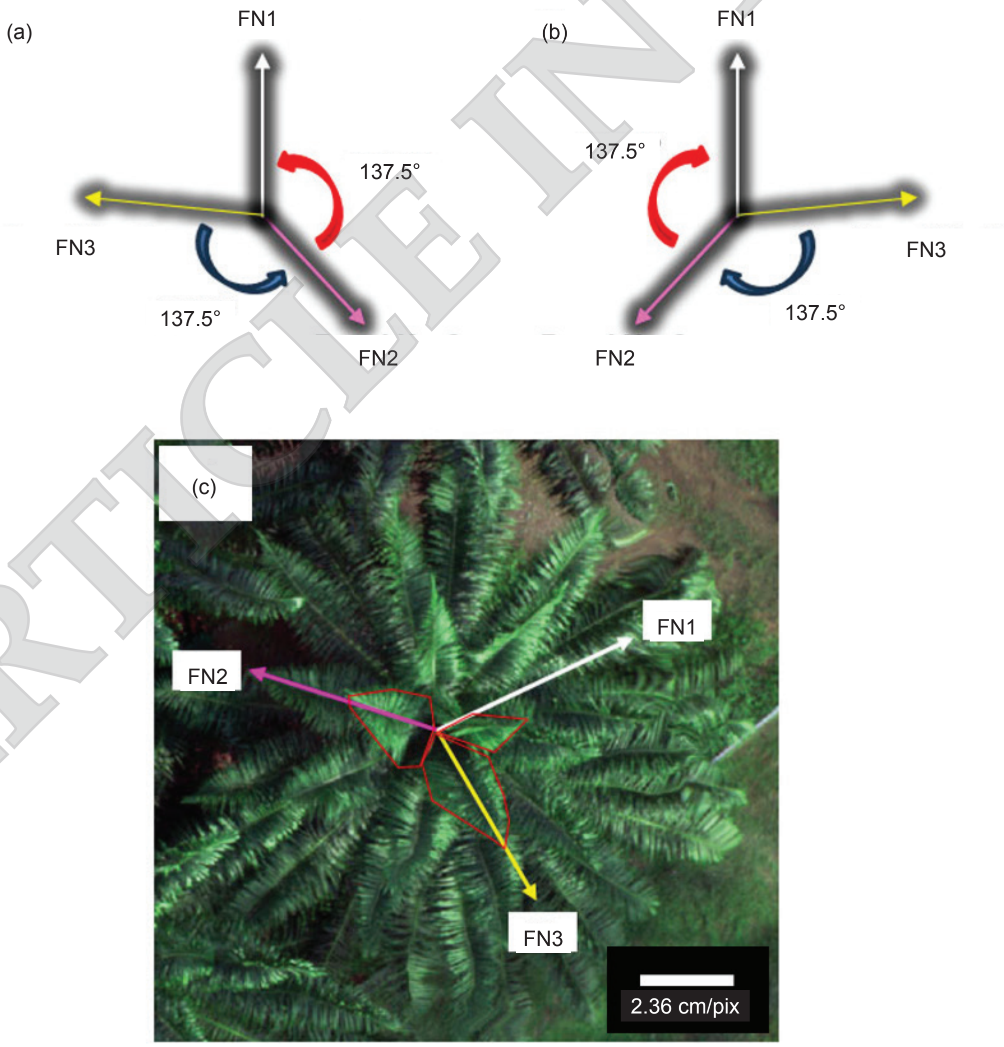

Figure 4. (a) Right-spiral 2DPIT for fronds number 1-3, (b) left-spiral 2DPIT for fronds 1-3, and (c) top-view of oil palm tree image with 2DPIT.

Application of 2DPIT on an oil palm tree aerial image. After establishing the optimal centre, the 2DPIT overlay process was implemented, tracing the sequence from FN3 to FN9. This approach enabled precise visualisation of divergence patterns based on the refined centre position. Using the overlaid template and corresponding image, we assessed the deviation between the template and the actual frond angle of FN1 and FN9.

Angular measurements of FN1 and FN9. After overlaying the image with 2DPIT, we calculated the angular deviation between the actual positions of FN1 and FN9 and compared them to their theoretical positions as illustrated in *Figure 5*. This measurement was performed using angular measurement tools in AutoCAD software (Autodesk, Inc., USA). The resulting deviations were then subjected to further statistical analysis to confirm the divergence angle at FN17, ensuring accuracy in identifying the phyllotaxis for the FN17 position.

Mathematical Modelling of Deviation Frond Angle

A mathematical model incorporating both quadratic and exponential elements was developed to represent the pattern of deviation angles from FN1 to FN17 for structural orientation across the canopy. Initial measurements of frond angle deviation were collected for FN1 and FN9 from both aerial and trunk positions across multiple planting blocks of varying age. These data points served as a foundation reference for creating an extrapolative model aimed at estimating the angular behaviour of FN17 and other intermediate frond numbers.

Validation of Frond Angle Deviation Models

To evaluate the accuracy of the predictive models, a validation process was conducted using the deviation angle of frond numbers not included in the original model fitting. Additional frond numbers, ranging from FN2 to frond number 8 (FN8), were chosen as validation points due to their structural significance and diverse canopy positions observed from top views. The Mean Absolute Error (MAE) and the Root Mean Square Error (RMSE) serve as indicators that quantify both the average and squared deviations between the observed and modelled outputs, thereby providing an objective basis for assessing model performance.

RESULTS AND DISCUSSION

Spiral Identification on Trunk

In a study involving 300 oil palm trees, the pseudo-bark position used to infer phyllotaxis patterns revealed that 158 displayed a right-handed spiral arrangement, while the remaining 142 exhibited a left-handed spiral arrangement. This spiral arrangement is crucial for capturing aerial images of oil palm tree canopies and for yield prediction. This finding is consistent with the study by Albakri et al. (2018), which indicates that the accurate prediction of FFB yield depends on identifying the tree's spiral arrangement. An overlay of 2DPIT was performed based on this preliminary data before conducting further angle analysis. Additionally, the phyllotaxis pattern on the stump was examined to verify the accuracy of the golden angle in an oil palm tree.

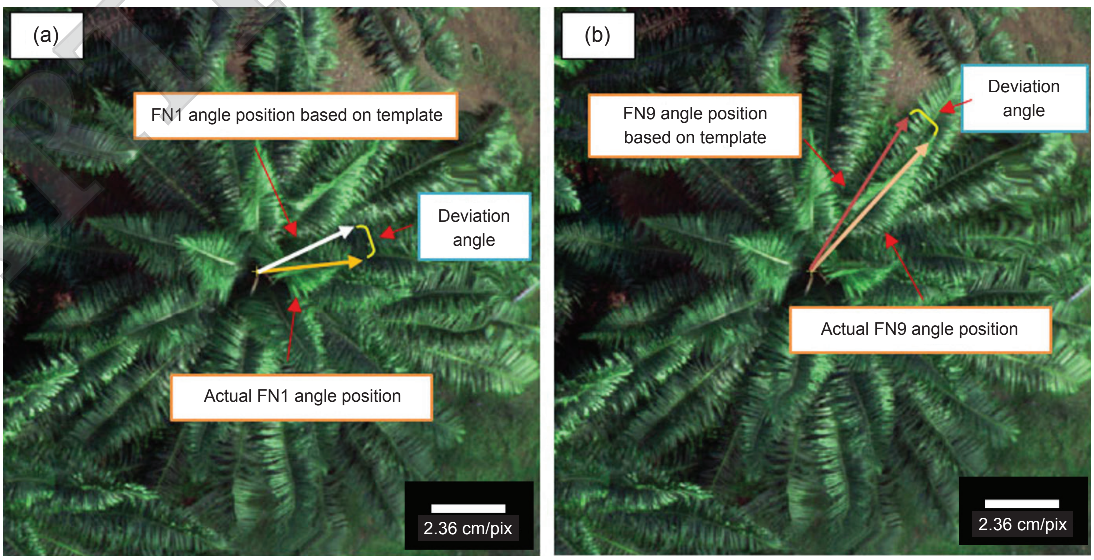

Figure 5. (a) Frond number 1 (FN1) and (b) frond number 9 (FN9) positions.

Stump Cross-section Analysis

A single tree was selected for crown cross-section analysis due to limitations in the availability of trees for sampling. Frond stump centres were identified using MATLAB version R2024b (MathWorks, Inc., USA). Straight lines were drawn from the canopy centre position on each frond stump. A portion of the crown cross-section was analysed to validate the findings reported by Okabe, (2015) and Guzman et al. (2022). Based on data from stump pattern analysis, the values generally converge toward this result of 137.5° from one stump to another (*Table 1*). The angular measurement increased by approximately 137.5° with each successive stump. For this study, a total of three full rotations (within a 360° framework) were required to determine the angular position of stump number five. The centre of the tree was labelled as zero, with the first stump deviating at the same angle by 137.5°. The differences between theoretical and actual measurements were minimal, deviating by −14.4° for the second, −2.2° for the third, −12.1° for the fourth and −12.6° for the fifth stump. This indicates that all the actual angles for stump measurement were consistently less than the theoretical angle prior to frond emergence. The deviation in angle is typical for planting trees, as the growth and positioning of oil palm fronds are influenced by factors such as soil and water availability (Prasetyo et al., 2024). The adaptive mechanism of the oil palm aims to optimise energy efficiency under varying environmental conditions (Alnuami et al., 2015).

Figure 6 illustrates the linear regression analysis of the actual deviation angle from FN1 to FN5 in relation to the theoretical golden angle of 137.5° for each frond deviation. The x-axis represents theoretical golden angles, while the y-axis displays the measured angles. Each data point corresponds to an individual leaf. The trendline is expressed by Equation (1), indicating a strong correlation as evidenced by an r^2 value of 0.9996.

$$y = 0.9819x - 0.6619 \qquad (1)$$

The high correlation suggests that the measured deviation angle aligns closely with theoretical values, underscoring the reliability of the measurement. This methodology aligns with the findings of Müller-Linow et al. (2015); Raabe et al. (2015) and Zou et al. (2014), who noted that variation in measured angle could arise from other factors, particularly environmental influence, which were not addressed in this study.

TABLE 1. STUMP MEASUREMENT

Frond number (*n*)	Total cycle (Mode 360°)	Theoretical angular (*TA*) (*n* x 137.5°)	Actual angular (*AA*) (°)	Differences (*TA – AA*) (°)	Result
0	0	0	0	0	None
1	1	137.5	137.5	0	None
2	1	275.0	260.6	–14.4	*TA* < *AA*
3	2	412.5	410.3	–2.2	*TA* < *AA*
4	2	550.0	537.9	–12.1	*TA* < *AA*
5	3	687.5	674.9	–12.6	*TA* < *AA*

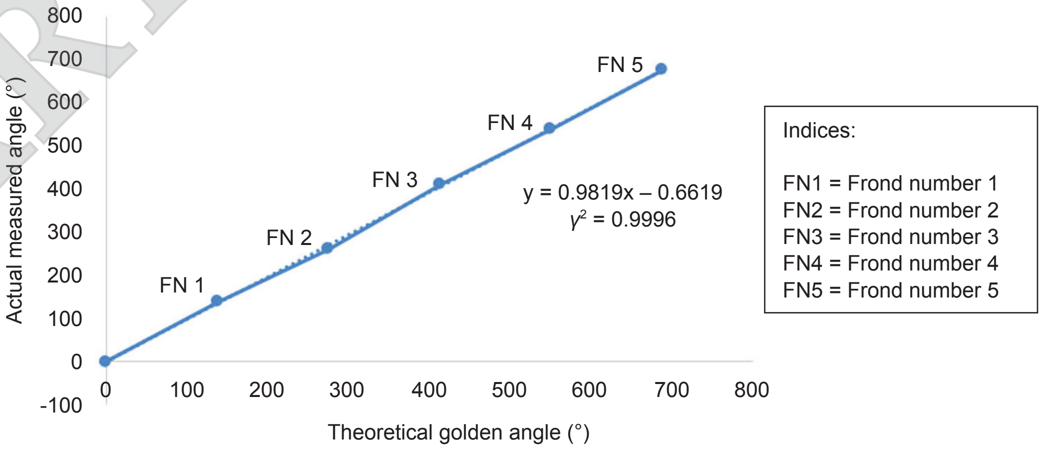

Figure 6. Linear regression of the actual measured angle vs. theoretical golden angle.

Angular Measurements of FN1 and FN9

The measured angles of FN1 and FN9 serve to indicate the deviation of fronds from the template toward the theoretically ideal angle of 137.5°. This deviation analysis study was essential for predicting the frond positioning within the oil palm canopy study. A mean comparison of the deviation angle for both aerial and ground FN1 and FN9 was conducted across different blocks, each with varying angle measurements. The analysis of variance (ANOVA) table (*Table 2*) presents the deviation angle (in degrees) for the aerial angle (AA) of the canopy and trunk angle (TA) pseudo-bank (formerly known as frond) for FN1 and FN9 across five blocks representing different oil palm ages post-planting. While no significant differences were observed among the blocks in terms of recorded angles, a significant interaction was found between block and angle, except for the aerial angle frond number nine (AAFN9).

TABLE 2. DEVIATION ANGLE OF AERIAL AND GROUND FN1 AND FN9 AT DIFFERENT BLOCKS WITH DIFFERENT ANGLE MEASUREMENTS

Item	AAFN1	AAFN9	TAFN1	TAFN9
ANOVA				
Block (B)	ns	ns	ns	ns
Angle (A)	ns	ns	ns	ns
B x A	*	ns	*	*
Block				
A (13 years after planting)	26.80[b]	7.62[a]	24.92[ab]	12.92[ab]
B (12 years after planting)	29.55[ab]	11.05[a]	20.33[b]	9.42[b]
C (15 years after planting)	32.10[a]	11.56[a]	29.83[ab]	14.92[a]
D (18 years after planting)	32.65[a]	12.75[a]	25.50[ab]	12.92[ab]
E (8 years after planting)	28.39[ab]	7.16[a]	33.25[a]	13.08[ab]
Mean (°)	**29.90**	**10.03**	**26.77**	**12.65**

Note: FN1 - frond number one; FN9 - frond number nine; AAFN1 - aerial angle frond number one; AAFN9 - aerial angle frond number nine; TAFN1 - trunk angle frond number one; TAFN9 - trunk angle frond number nine; ANOVA - analysis of variance; ns - no significant difference; * - significant at $p < 0.05$; Means with different letters vertically within each age at different blocks are significantly different.

For AAFN1, the highest recorded angle was observed in Block D at 32.65°, while Block A had the lowest at 26.80°. Block C and D exhibited significantly higher values compared to Block A, suggesting variation in deviation patterns with age. In contrast, AAFN9 showed no significant differences, indicating generally similar deviations across the blocks. The highest angle for AAFN9 was measured at Block D, at 12.75°, with a minimum angle of 7.16° recorded in Block E. In TAFN1, Block E had the highest angle at 33.25°, whereas Block B had the lowest at 20.33°.This highlights a substantial difference between Block E and B, with Block C displaying values closer to those of Block E. Conversely, for TAFN9, the highest deviation angle was noted in Block B at 14.92°. In comparison, the lowest angle was also recorded on Block B at 9.42°, which mirrors the finding of TAFN1.

Analysis of deviation angles across different age groups of the plantation revealed variation in frond orientation. This study supports the finding of Khairuniza-Bejo et al. (2015), which indicated that differing angles of oil palm fronds yield distinct results, particularly concerning disease detection. Notably, AAFN1 displayed the highest mean values, suggesting a greater angular displacement when viewed aerially, particularly for the first frond compared to the measurement's subsequent fronds and trunk. Conversely, AAFN9 exhibits the least deviation at 10.03°, indicating a more upright growth pattern in the later frond.

Although ANOVA indicated no statistically significant differences across the blocks, the interaction between blocks and angle highlighted meaningful trends. Block D, assessed 18 years after planting, consistently displayed higher deviation angles when measured through aerial images. This suggests a potential peak in structural deviation driven by age-related growth dynamics. In contrast, the analysis of ground images of the trunk and pseudo-bark revealed that Block B had a lower angle, likely reflecting greater vertical structural integrity among mid-aged oil palm trees. This study is consistent with the findings of Husin et al. (2020), who used ground-based light detection and ranging (LiDAR) to monitor basal stem rot (BSR), indicating that a larger frond angle correlates with a smaller crown area and a reduced number of fronds observed. The results suggest that the angle of fronds is affected by both the number of fronds and the age of the block, with the most significant deviation likely occurring around 18 years after planting. These insights are valuable for understanding mechanical stability and enhancing light interception in oil palm plantations.

Mathematical Modelling of Deviation Frond Angle

A mathematical model was created to explore the relationship between the deviation angles of aerial fronds and the increasing number of fronds in oil palm trees. The analysis was designed to simulate the anticipated angular divergence, based on the assumption that the deviation angles decrease exponentially. *Figure 7* presents a step-by-step comparison of the modelling process for both quadratic and exponential models.

The initial step involved utilising the raw data to construct a linear model (*Figure 7a*). To develop the second-degree polynomial model, a quadratic equation was applied, which was derived from FN1 and FN9 data of the earlier linear model presented in *Figure 7a*. However, this model tends to overfit to the limited amount of data available. The Equation (2) referenced is;

$$\theta(n) = an^2 + bn + c \qquad (2)$$

where, $\theta(n)$ represents the frond deviation angle in degrees and n is the frond number. The coefficients a, b and c were obtained using the measured deviation aerial data of FN1 and FN9, as illustrated in *Figure 7b*. However, due to the limited number of data points, as we only measured two frond positions (FN1 referred to as a and FN9 as b), there was insufficient data to support a quadratic extrapolation for point c.

To overcome this limitation, the exponential model was reformulated into a linear format by applying the natural logarithm to angle values, allowing for a straight-line fit as shown in *Figure 7c*. This approach facilitated the development of the final exponential decay model (*Figure 7d*), which accurately reflects the natural decay trend of frond angle divergence and proved to be more effective for angle prediction. The model is expressed as shown in Equation (3):

$$\theta(n) = A \times e^{-kn} \qquad (3)$$

where, A and k are empirical constants derived from the simulated aerial data of FN1 and FN9, based on observed trends in frond orientation. These constants are calculated using Equation (4) and Equation (5), respectively:

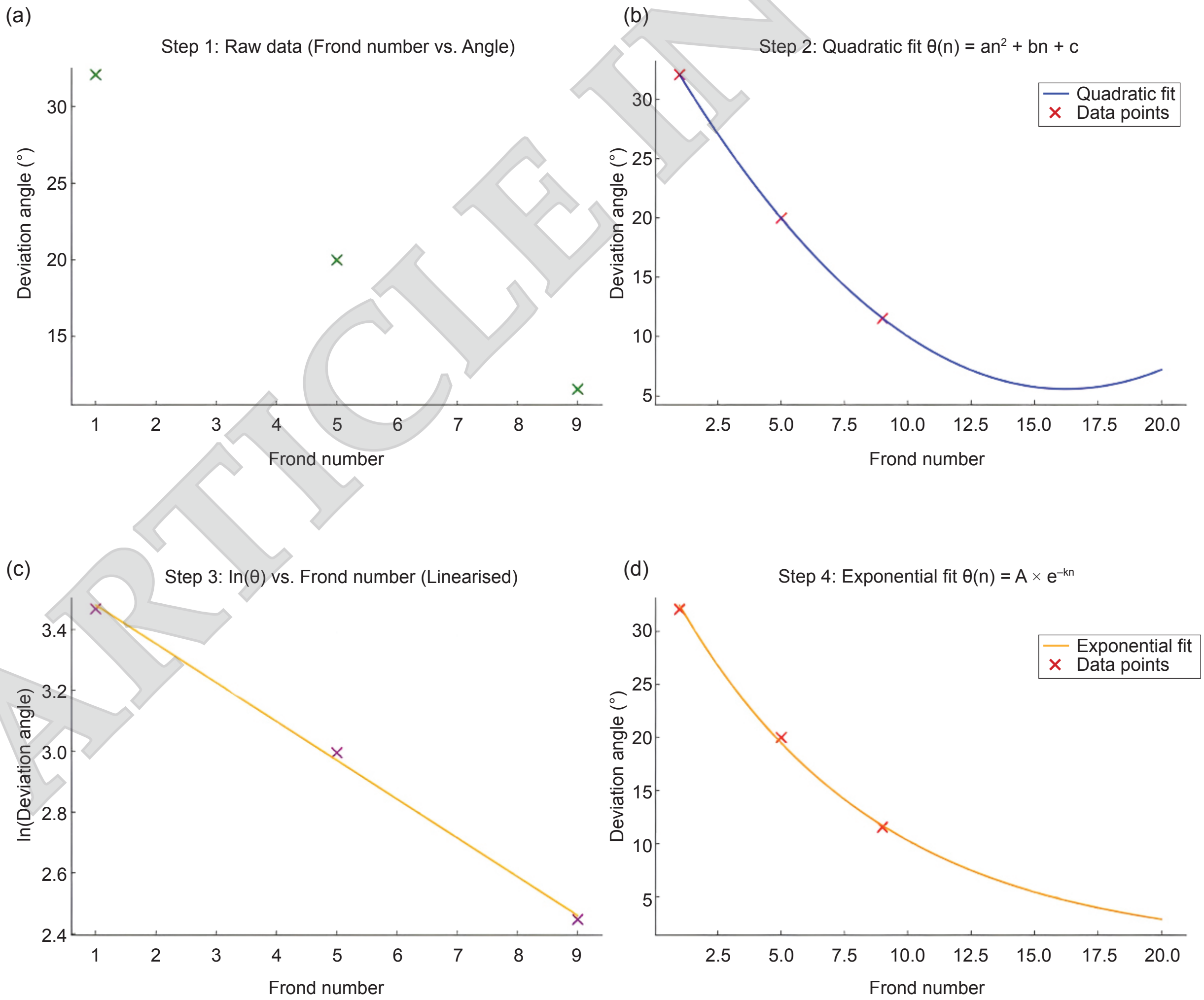

Figure 7. Modelling equation process across frond numbers and deviation angle.

$$\text{Average } A\text{: } A\,(\text{age}) = \begin{matrix}(0.01238 \text{ x age}^2) - \\ (0.11841 \text{ x age}) + \\ 35.50989\end{matrix} \quad (4)$$

$$\text{Average } k\text{: } k\,(\text{age}) = \begin{matrix}(0.00156 \text{ x age}^2) - \\ (0.04691 \text{ x age}) + \\ 0.48063\end{matrix} \quad (5)$$

Validation of Frond Angle Deviation Models

For the validation process, 60 oil palm tree samples were randomly selected from 30 right-handed spiral fronds and 30 left-handed spiral fronds, chosen for their structural significance and diverse canopy positions. To evaluate the accuracy and predictive reliability of the developed models for the quadratic and exponential models, a validation process was conducted using deviation angle measurements from frond numbers not included in the original model fitting. Specifically, FN2 toward FN8 were selected as validation points due to their structural significance and varied canopy positions from aerial views. Predictions were generated using these independently measured angles based on the exponential decay model.

Table 3 below presents a comparison of standard deviation (SD), 95% confidence interval (CI), mean absolute error (MAE) and root mean square error (RMSE) for predicting the frond spiral angle using the spiral model. The performance of the spiral phyllotaxis-based model was assessed separately for right- and left-handed spiral patterns to evaluate its directional prediction capability. For the right-handed spiral, the model achieved an MAE of 3.02° and an RMSE of 3.85°, reflecting a relatively low discrepancy between the predicted and actual frond angles. In contrast, the left-handed spiral has higher values, with an MAE of 3.94° and an RMSE of 4.76°.

The statistical metrics used in this study serve two different purposes. MAE and RMSE are applied as performance indicators to evaluate the accuracy of the spiral model predictions. At the same time, SD and 95% CI are used to describe the variability and uncertainty of the predicted frond spiral angles. The measured angular values displayed moderate variability across different frond positions. For the right-handed spiral, the SD was observed to range from ±3.30° to ±8.29°, reflecting biological variations from the ideal golden-angle divergence due to factors such as frond growth dynamics, canopy asymmetry and age-related structural adjustments. In contrast, the left-handed spiral exhibited SD between ±3.93° and ±9.29°, indicating a slightly greater dispersion influenced by elements such as spiral orientation effects, varying frond exposure and heightened sensitivity to image-based angular distortion.

TABLE 3. EVALUATION OF FROND SPIRAL ANGLE PREDICTION USING MAE, RMSE AND VARIABILITY METRICS

Right-spiral arrangement of the oil palm tree						
Frond number (FN)	**Measured angle (°)**	**Predicted angle (°)**	**Standard deviation (SD) (±°)**	**95% Confidence interval (CI) (°)**	**Absolute angle error (°)**	**Squared angle error (°²)**
FN2	23.75	27.87	±7.71	18.58–28.92	4.13	17.03
FN3	20.90	24.32	±7.84	15.75–25.71	3.42	11.73
FN4	20.52	21.22	±7.28	16.09–24.89	0.71	0.50
FN5	19.31	18.53	±6.16	15.74–22.54	0.78	0.61
FN6	15.89	16.19	±3.30	12.38–17.90	0.30	0.09
FN7	18.57	14.17	±8.29	13.58–22.76	4.40	19.33
FN8	19.83	12.44	±7.24	16.47–24.48	7.39	54.59
Mean					**(MAE) 3.02**	**(RMSE) 3.85**
Left-spiral arrangement of the oil palm tree						
Frond number (FN)	**Measured angle (°)**	**Predicted angle (°)**	**Standard deviation (SD) (±°)**	**95% Confidence interval (CI) (°)**	**Absolute angle error (°)**	**Squared angle error (°²)**
FN2	18.58	27.87	±9.29	8.82–28.34	9.29	86.32
FN3	19.43	24.32	±8.39	16.21–25.49	4.89	23.94
FN4	18.11	21.22	±8.98	13.64–23.24	3.12	9.72
FN5	18.69	18.53	±8.74	13.64–23.24	0.16	0.03
FN6	14.51	16.19	±3.93	11.25–16.87	1.68	2.81
FN7	18.90	14.17	±6.86	15.94–23.86	4.73	22.36
FN8	16.16	12.44	±7.73	12.81–20.49	3.72	13.86
Mean					**(MAE) 3.94**	**(RMSE) 4.76**

Note: MAE - mean absolute error; RMSE - root mean square error.

The 95% CI indicates stable central tendencies across frond positions. For right-handed spirals, the confidence intervals were well-defined (e.g., FN6: 11.25°–16.87°), despite the inequalities in sample sizes due to partial data availability. This suggests that the fundamental geometry of the spiral significantly influences the angular distribution of the fronds. Likewise, left-handed spirals exhibited relatively narrow confidence intervals for most fronds (e.g., FN6: 12.38°–17.90°), reflecting a consistent central tendency influenced by the same phyllotactic principles. The convergence of confidence interval widths in both spiral orientations further reinforce the credibility of the proposed aerial imagery-based frond angle modelling approach, highlighting its robustness in addressing data gaps and sampling disparities in real plantation settings.

The close MAE values suggest that the average prediction errors in both spiral directions are similar, indicating a consistent model performance regarding absolute deviations. MAE is frequently regarded as a straightforward measure of model accuracy due to its equal weighting of all errors (Hodson, 2022). In contrast, the elevated RMSE associated with the left-handed spiral, which places greater emphasis on larger errors, suggests the presence of outliers or irregular angular deviations as noted by Chai and Draxler (2014). This may be attributed to natural variability in the development of spiral, inconsistent frond visibility using UAV-based imagery, or potential error propagation from angle detection algorithms.

The advancement of convolutional neural networks (CNNs) has proven highly effective in detecting oil palm leaves, particularly for applications such as disease diagnosis (Ong et al., 2022; Septiarini et al., 2022) and identifying nutrient deficiencies (Razali et al., 2022). These networks rely heavily on large, labelled datasets and appearance-based features. However, CNNs primarily concentrate on classification rather than the spatial arrangement of fronds within the canopy. In contrast, our study employed the 2DPIT, which utilises a geometry-driven approach to establish the positional order of fronds based on the natural spiral phyllotaxis observed in oil palms. This methodology does not require extensive training data or complex optimisations; instead, it utilises deterministic angular relationships, which enable robustness against variations in environmental conditions. 2DPIT effectively addresses a notable limitation of CNNs by offering a consistent reference for frond numbering, which is essential for nutrient sampling and physiological studies. While CNNs excel in visual classification, 2DPIT contributes additional value by providing a stable, interpretable framework that can enhance automated detection systems within precision plantation management and research.

A previous study by Culman et al. (2020) demonstrated the effectiveness of CNNs for detecting individual palm trees from high-resolution RGB aerial imagery, achieving impressive detection accuracy across diverse landscapes. However, their approach was mainly focused on spatial inventory and did not extend to the extraction of structural canopy parameters. In contrast, the present study builds on this detection framework by incorporating morphological analysis, specifically frond angle modelling, which offers deeper insight into canopy architecture and the physiological status of the plants. This evolution from object detection to structural phenotyping highlights the potential of aerial imagery not only for mapping but also for functional trait analysis in oil palm systems.

Recent advances in deep learning have significantly improved the capability for individual tree-level analysis using high-resolution imagery. For instance, Freudenberg et al. (2022) developed a U-Net-based framework for individual tree crown delineation, enabling the extraction of tree crown polygons from aerial and satellite imagery without requiring LiDAR data. Their approach demonstrates that accurate tree-level segmentation can be achieved using only two-dimensional (2D) optical imagery, supporting the feasibility of cost-effective large-scale monitoring. This is highly relevant to oil palm plantations, where individual palm detection forms the basis for yield estimation and structural analysis. However, their findings also highlight challenges in separating closely spaced or small crowns, which are common in dense plantation settings. In contrast, the present study focuses on structured frond-based detection, which may provide additional robustness in identifying individual palms even under overlapping canopy conditions.

In the findings of S. Zhang et al. (2025), they created the STEM-OP framework, which effectively extracts single trees in Malaysia, emphasising the importance of this information for regional analysis. While their focus is on mapping and counting, our study uses single-palm delineation as a prerequisite for analysing oil palm phyllotaxis. Isolating individual trees enables accurate extraction of frond positions, which are essential for modelling divergence angles with the exponential decay model. Our findings extend the value of single-tree detection beyond spatial mapping to biological interpretation, validating phyllotactic patterns consistent with theoretical spiral growth and aiding in estimating key frond positions, such as FN17. This marks a shift from mere spatial analysis to a deeper integration of geometric and physiological understanding in oil palm studies.

A similar study was conducted in Honduras to detect individual oil palm trees and assess their potential for expansion, as reported by H. Zhang et al. (2025). Their works demonstrated the effectiveness of submeter-resolution RGB imagery for analysing oil palm in Honduras, detecting individual trees and assessing spatial distribution using methods such as four-direction gradient difference (FGD) and double-ring techniques. The approach achieved impressive accuracy, with an F1-score of 86.53% and estimated that there are 0.25 million hectares of plantations, corresponding to approximately 28.27 million trees with an average density of 113 trees/ha. These findings affirm the ability of high-resolution imagery to capture oil palm canopy morphology at the individual-tree level. Although their study primarily focused on detection and large-scale mapping, it lays a methodological foundation for enhancing remote sensing applications toward more detailed structural analysis. In this context, the current study builds on their work by modelling frond angle variation using an exponential decay function, enabling a more nuanced characterisation of within-canopy architecture.

Palm-specific detection approaches further support the applicability of 2D-based methodologies for individual plant analysis. For example, Dos Santos et al. (2017) demonstrated the feasibility of automatically detecting babassu palms using very high-resolution satellite imagery through object-based image analysis and crown pattern recognition. Their results show that palm trees can be reliably identified from their distinctive radial crown structure in 2D imagery, even without three-dimensional (3D) information. This is directly relevant to the present study, which also exploits the geometric configuration of oil palm crowns using the proposed 2D-PIT framework. However, while their approach focuses primarily on crown-level detection for density estimation, the present study extends this concept by incorporating frond-level spatial information and phyllotactic structure, enabling a more detailed representation of individual palm architecture.

Wibowo et al. (2022) demonstrated that UAV-based deep learning techniques, especially Mask R-CNN, effectively detect and segment individual oil palm crowns from high-resolution images. This capability provides reliable tree-level information, essential for precision agriculture, including monitoring and inventory management. Building on this, the current study uses single-palm delineation for structural analysis, allowing accurate isolation of each crown and identification of fronds. This precision is crucial for modelling divergence angles with the exponential decay model. Building on the accuracy of Wibowo et al. (2022), this study further explores oil palm phyllotaxis, examining spiral growth behaviour and estimating key frond positions within a golden-angle framework, showcasing the potential of single-palm detection for geometric modelling.

To enhance the practical application of the proposed frond detection method, it can be effectively integrated as a fundamental element within a hierarchical, tree-level remote sensing workflow. This comprehensive process generally comprises four key stages: (1) Individual tree detection, (2) crown delineation, (3) intra-crown frond detection and (4) temporal monitoring at the tree level.

At the first stage, individual oil palm trees are automatically detected from UAV or very high-resolution imagery using object detection or crown localisation approaches such as CNNs or template matching. The output of this step is a set of georeferenced tree locations (centroids), which define the spatial units for subsequent analysis. This ensures that all downstream processing is performed at the individual-tree level rather than at the pixel level.

Following detection, crown delineation is performed to segment the spatial extent of each palm canopy. This can be achieved using methods such as watershed segmentation, region growing, or deep learning-based instance segmentation. The delineated crown boundary constrains the area of interest, effectively isolating each tree and reducing interference from neighbouring palms, understory vegetation, or background noise.

Within each segmented crown, the proposed frond detection method is then applied as a fine-scale structural analysis module. Using the identified crown centre as a reference point, the method enables the detection of frond positions, the estimation of angular relationships such as FN1–FN9 deviation and subsequent frond arrangement modelling. The output consists of frond-level features, including frond count, angular distribution and potentially frond-specific spectral responses. These frond-level metrics can then be aggregated to derive tree-level attributes. For instance, frond count and spatial arrangement can serve as proxies for palm age, vigour and structural health, while spectral signatures associated with individual fronds can support nutrient status or stress detection. This enables the transition from structural detection to functional interpretation at the tree scale.

Finally, when multi-temporal UAV datasets are available, the workflow supports longitudinal monitoring of individual trees. By consistently tracking the same tree IDs across time, changes in frond number, emergence patterns, or angular deviations can be analysed to quantify growth dynamics, detect anomalies such as missing or damaged fronds and improve yield forecasting models. This temporal component is particularly valuable for precision agriculture applications, where early detection of stress or suboptimal growth can inform targeted interventions.

In summary, the proposed frond detection approach is not a standalone technique but a scalable module within a comprehensive tree-level monitoring framework. Its integration bridges the gap between crown-level segmentation and high-level agronomic insights, enabling detailed phenotyping of oil palms from UAV imagery and supporting advanced plantation management strategies.

This study illustrates that UAV-derived frond angle modelling can effectively characterise the phyllotaxis of oil palm, even during the structural asymmetry observed between left- and right-handed spirals. While right-handed spirals showed marginally higher predictive accuracy, which aligned with their natural prevalence in oil palm trees, the integration of a geometric divergence-angle template alongside image-derived measurements significantly reduces directional bias. The combined use of predicted phyllotactic positions enabled reliable detection of frond number, effectively addressing challenges related to canopy occlusion, frond overlap and irregular crown morphology. This methodological advancement overcomes a critical limitation in automated frond sequencing by offering an objective and repeatable reference for frond count across various tree ages and crown structures.

CONCLUSION

The operational scope of the proposed 2DPIT is primarily focused on frond-level identification and structural analysis within already-detected individual oil palm crowns, rather than serving as a standalone palm detection approach. Specifically, 2DPIT is designed to model the angular arrangement of fronds based on phyllotactic principles, enabling the identification of key fronds such as FN1 and FN9 and the quantification of deviation angles from the expected spiral pattern. As such, the method assumes that individual palms have been pre-localised using existing approaches, such as high-resolution UAV imagery, object-based image analysis, or deep learning-based crown-detection frameworks. Using this information, FN17 can be precisely located, thereby minimising bias in nutritive frond sampling decisions made by ground-view agronomists. An exponential decay model has been developed and validated, demonstrating strong predictive capabilities, especially for oil palm trees exhibiting right-handed spirals, which are predominant in oil palm growth. Although left-handed spirals showed slightly higher error margins, the model remains largely applicable and versatile. The findings indicate that frond angle deviation is correlated with both frond number and tree age, with peak structural deviation occurring approximately 18 years after planting in this study. The combination of aerial imagery, phyllotactic modelling, and angle validation provides groundwork for accurate, non-destructive frond identification. Overall, the proposed method is not intended to replace existing palm detection or mapping techniques, but rather to extend their capabilities by enabling fine-scale, biologically meaningful analysis at the frond level. This integration enhances the applicability of UAV-based remote sensing for precision plantation management and supports more comprehensive tree-level monitoring strategies.

Future research should focus on incorporating machine-learning techniques for automated frond segmentation, developing spiral-type calibration algorithms to enhance left-handed accuracy, and integrating temporal UAV monitoring to observe the dynamics of crown development. The utilisation of multisensor data, including multispectral, thermal and LiDAR, can further improve diagnostics of canopy health and stress detection. The future of 3D modelling promises transformative possibilities that inspire creativity and innovation in specific frond detection. As technology evolves, we can anticipate an exciting landscape in which agronomists and engineers alike will harness advanced tools and techniques to deliver better outcomes, especially in oil palm monitoring. This approach ultimately promotes more intelligent, data-driven plantation management, advancing precision agriculture in the oil palm sector. By enhancing the accuracy of frond detection, we directly strengthen smarter plantation management. Improved frond referencing enables more precise nutrient diagnosis, optimises pruning and harvesting decisions, facilitates early identification of plant stress and enhances yield forecasting. By enabling consistent, scalable and automated assessments of the canopy, this method positions UAV-based phyllotaxis modelling as a vital element of the next generation of precision agriculture in the oil palm industry.

ACKNOWLEDGEMENT

We express our sincere gratitude to the Putra Agriculture Center in Malaysia for granting approval for this project. This support has not only made our current study viable but has also significantly enhanced its overall vibrancy.

REFERENCES

Ahmad, M. N., Sharif, A. R. M., & Moslim, R. (2025). The functionality and features of the AI automated detector and counter, Oto-BaC™ for bagworm census in oil palm plantation. *Indian Journal of Engineering and Materials Sciences (IJEMS), 31*(6), 914–921. https://doi.org/10.56042/ijems.v31i6.10931

Ahmad, M. J., Ismail, R., Kamarulzaman, N. H., & Ghani, F. A. (2024). Socio-economic impacts of oil palm plantations in Malaysia: A review of economic and environmental perspectives. *Advanced International Journal of Business, Entrepreneurship and SME's, 6*(20), 319–330. https://doi.org/10.35631/aijbes.620026

Ahmadi, P., Mansor, S., Farjad, B., & Ghaderpour, E. (2022). Unmanned aerial vehicle (UAV)-based remote sensing for early-stage detection of *Ganoderma*. *Remote Sensing*, *14*(5), 1239. https://doi.org/10.3390/rs14051239

Ahmadi, P., Muharam, F. M., Ahmad, K., Mansor, S., & Seman, I. A. (2017). Early detection of *Ganoderma* basal stem rot of oil palms using artificial neural network spectral analysis. *Plant Disease*, *101*(6), 1009–1016. https://doi.org/10.1094/pdis-12-16-1699-re

Ali, M. M., Bachik, N. A., Muhadi, N. A., Yusof, T. N. T., & Gomes, C. (2019). Non-destructive techniques of detecting plant diseases: A review. *Physiological and Molecular Plant Pathology*, *108*, 101426. https://doi.org/10.1016/j.pmpp.2019.101426

Ali, M. S., Vaiappuri, S. K. N., & Tariq, S. (2024). Malaysian oil palm industry: A view on the economic, social, and environmental aspects. In C. Popescu, J. Martínez-Falcó, B. Marco-Lajara, E. Sánchez-García, & L. Millán-Tudela (Eds.), *Economics and environmental responsibility in the global beverage industry* (pp. 268–284). IGI Global. https://doi.org/10.4018/979-8-3693-2149-2.ch014

Alnuami, W., Janius, R. B., Ahmad, D., Akhir, M., & Buthainah, A. (2015). Factors affecting the mechanical strengths of oil palm fronds. *Journal of Purity, Utility, Reaction and Environment*, *4*(3), 138–149.

Albakri, Z. M., Kassim, M. S. M., Abdullah, A. F., & Harith, H. H. (2019). Analysis of oil palm leaf phyllotaxis towards development of models to determine the fresh fruit bunch (FFB) maturity stages, yield and site-specific harvesting. *Pertanika Journal of Science & Technology, 27*(2), 659–672.

Amirruddin, A. D., Muharam, F. M., Ismail, M. H., Ismail, M. F., Tan, N. P., & Karam, D. S. (2020a). Hyperspectral remote sensing for assessment of chlorophyll sufficiency levels in mature oil palm (*Elaeis guineensis*) based on frond numbers: Analysis of decision tree and random forest. *Computers and Electronics in Agriculture*, *169*, 105221. https://doi.org/10.1016/j.compag.2020.105221

Amirruddin, A. D., Muharam, F. M., Ismail, M. H., Tan, N. P., & Ismail, M. F. (2020b). Hyperspectral spectroscopy and imbalance data approaches for classification of oil palm's macronutrients observed from frond 9 and 17. *Computers and Electronics in Agriculture*, *178*, 105768. https://doi.org/10.1016/j.compag.2020.105768

Asyraf, M. R. M., Ishak, M. R., Syamsir, A., Nurazzi, N. M., Sabaruddin, F. A., Shazleen, S. S., Norrrahim, M. N. F., Ilyas, R. A., Rashid, M. Z. A., & Razman, M. R. (2022). Mechanical properties of oil palm fibre-reinforced polymer composites: A review. *Journal of Materials Research and Technology*, *17*, 33–65. https://doi.org/10.1016/j.jmrt.2021.12.122

Avtar, R., Suab, S. A., Syukur, M. S., Korom, A., Umarhadi, D. A., & Yunus, A. P. (2020). Assessing the influence of UAV altitude on extracted biophysical parameters of young oil palm. *Remote Sensing*, *12*(18), 3030. https://doi.org/10.3390/rs12183030

Azuan, N. H., Khairunniza-Bejo, S., Abdullah, A. F., Kassim, M. S. M., & Ahmad, D. (2019). Analysis of changes in oil palm canopy architecture from basal stem rot using terrestrial laser scanner. *Plant Disease*, *103*(12), 3218–3225. https://doi.org/10.1094/pdis-10-18-1721-re

Breure, C. J. (1985). Relevant factors associated with crown expansion in oil palm (*Elaeis guineensis* Jacq.). *Euphytica*, *34*, 161–175. https://doi.org/10.1007/BF00022876

Breure, C. J. (1994). Development of leaves in oil palm (*Elaeis guineensis*) and determination of leaf opening rate. *Experimental Agriculture*, *30*(4), 467–472. https://doi.org/10.1017/S0014479700024728

Chai, T., & Draxler, R. R. (2014). Root mean square error (RMSE) or mean absolute error (MAE)? – Arguments against avoiding RMSE in the literature. *Geoscientific Model Development*, *7*(3), 1247–1250. https://doi.org/10.5194/gmd-7-1247-2014

Corley, R. H. V., & Tinker, P. B. (2015). *The oil palm* (5th ed.). Wiley Blackwell.

Culman, M., Delalieux, S., & Van Tricht, K. (2020). Individual palm tree detection using deep learning on RGB imagery to support tree inventory. *Remote Sensing*, *12*(21), 3476. https://doi.org/10.3390/rs12213476

Daou, L., Garnier, É., & Shipley, B. (2021). Quantifying the relationship linking the community-weighted means of plant traits and soil fertility. *Ecology*, *102*(9), e03454. https://doi.org/10.1002/ecy.3454

De Mello Prado, R., & Rozane, D. E. (2020). Leaf analysis as diagnostic tool for balanced fertilization in tropical fruits. In A. K. Srivastava & C. Hu (Eds.), *Fruit crops: Diagnosis and management of nutrient constraints* (pp. 131–143). Elsevier. https://doi.org/10.1016/B978-0-12-818732-6.00011-3

Dos Santos, A. M., Mitja, D., Delaître, E., Demagistri, L., De Souza Miranda, I., Libourel, T., & Petit, M. (2017). Estimating babassu palm density using automatic palm tree detection with very high spatial resolution satellite images. *Journal of Environmental Management*, *193*, 40–51. https://doi.org/10.1016/j.jenvman.2017.02.004

Formaglio, G., Veldkamp, E., Damris, M., Tjoa, A., & Corre, M. D. (2021). Mulching with pruned fronds promotes the internal soil N cycling and soil fertility in a large-scale oil palm plantation. *Biogeochemistry*, *154*, 63–80. https://doi.org/10.1007/s10533-021-00798-4

Freudenberg, M., Magdon, P., & Nölke, N. (2022). Individual tree crown delineation in high-resolution remote sensing images based on U-Net. *Neural Computing and Applications*, *34*, 22197–22207. https://doi.org/10.1007/s00521-022-07640-4

Givnish, T. J. (1987). Comparative studies of leaf form: Assessing the relative roles of selective pressures and phylogenetic constraints. *New Phytologist*, *106*(S1), 131–160. https://doi.org/10.1111/j.1469-8137.1987.tb04687.x

Guzmán, E., Fernández, M. P., Alcalde, J. A., Contreras, S., Raumonen, P., Picco, L., Montalba, C., & Tejos, C. (2022). Phyllotaxis transition over the lifespan of a palm tree using Magnetic Resonance Imaging (MRI) and Terrestrial Laser Scanning (TLS): The case of *Jubaea chilensis*. *Plant Methods*, *18*(1), 88. https://doi.org/10.1186/s13007-022-00920-z

Hariadi, B., Sastrohartono, H., Krisdiarto, A. W., Sukarman, S., Primananda, S., & Sagoro, T. H. (2024a). The prediction of nitrogen, phosphate, and potassium contents of oil palm leaf using hand-held spectrometer. *Jurnal Teknik Pertanian Lampung*, *13*(1), 71–81. https://doi.org/10.23960/jtep-l.v13i1.71-81

Hariadi, B., Sastrohartono, H., Krisdiarto, A. W., Sukarman, S., Sagoro, T. H., Primananda, S., Akbar, A. R. M., & Uktoro, A. I. (2024b). The use of the Normalized Difference Red Edge (NDRE) vegetation index from multispectral cameras mounted on unmanned aerial vehicle to estimate the nutrient content in oil palm leaves. *Jurnal Teknik Pertanian Lampung (Journal of Agricultural Engineering)*, *13*(4), 1051–1063. https://doi.org/10.23960/jtep-l.v13i4.1051-1063

Herman, M. S., Hashim, F. H., Zulkifli, Z. M., Huddin, A. B., & Salim, G. M. (2024). Oil palm leaves phenotyping using biomarkers derived from Raman spectra. *Malaysian Journal of Fundamental and Applied Sciences*, *20*(1), 10–20. https://doi.org/10.11113/mjfas.v20n1.3139

Hodgson, J. G., Montserrat-Martí, G., Charles, M., Jones, G., Wilson, P., Shipley, B., Sharafi, M., Cerabolini, B. E. L., Cornelissen, H. C., Band, S. R., Bogard, A., Castro-Díez, P., Guerrero-Campo, J., Palmer, C., Pérez-Rontomé, M. C., Carter, G., Hynd, A., Romo-Díez, A., de Torres Espuny, L., & Royo Pla, F. (2011). Is leaf dry matter content a better predictor of soil fertility than specific leaf area? *Annals of Botany*, *108*(7), 1337–1345. https://doi.org/10.1093/aob/mcr225

Hodson, T. O. (2022). Root mean square error (RMSE) or mean absolute error (MAE): When to use them or not. *Geoscientific Model Development*, *15*(14), 5481–5487. https://doi.org/10.5194/gmd-15-5481-2022

Husin, N. A., Khairunniza-Bejo, S., Abdullah, A. F., Kassim, M. S. M., Ahmad, D., & Azmi, A. N. N. (2020). Application of ground-based LiDAR for analysing oil palm canopy properties on the occurrence of basal stem rot (BSR) disease. *Scientific Reports*, *10*(1), 6464. https://doi.org/10.1038/s41598-020-62275-6

Janani, M., & Jebakumar, R. (2022). Analysis of leaf nutrient concentration in different crop species using image processing techniques. In *2022 Fourth International Conference on Emerging Research in Electronics, Computer Science and Technology (ICERECT)* (pp. 1–7). IEEE. https://doi.org/10.1109/ICERECT56837.2022.10060282

Jayaselan, H. A. J., Nawi, N. M., Ismail, W. I. W., Shariff, A. R. M., Rajah, V. J., & Arulandoo, X. (2017). Application of spectroscopy for nutrient prediction of oil palm. *Journal of Experimental Agriculture International*, *15*(3), 1–9. https://doi.org/10.9734/JEAI/2017/31502

Khairy, R. N., & Syafi'i, W. (2025). Literature analysis of phylotaxis pattern variation in plants: Symmetry, classification, and species representation. *Bio-Lectura: Jurnal Pendidikan Biologi*, *12*(1), 127–137. https://doi.org/10.31849/bl.v12i1.26737

Khairunniza-Bejo, S., Yusoff, Y., Yusoff, N. S. N., Seman, I. A., & Anuar, M. I. (2015). Identification of healthy and BSR-infected oil palm trees using color indices. *International Journal of Agricultural and Biosystems Engineering*, *9*(8), 876–879.

Khuzaimah, Z., Nawi, N. M., Adam, S. N., Kalantar, B., Emeka, O. J., & Ueda, N. (2022). Application and potential of drone technology in oil palm plantation: Potential and limitations. *Journal of Sensors*, *2022*, 5385505. https://doi.org/10.1155/2022/5385505

Kok, Z. H., Shariff, A. R. B. M., Khairunniza-Bejo, S., Kim, H. T., Ahamed, T., Cheah, S. S., & Wahid, S. A. A. (2021). Plot-based classification of macronutrient levels in oil palm trees with Landsat-8 images and machine learning. *Remote Sensing*, *13*(11), 2029. https://doi.org/10.3390/rs13112029

Kouadio, L., El Jarroudi, M., Belabess, Z., Laasli, S.-E., Roni, M. Z. K., Amine, I. D. I., Mokhtari, N., Mokrini, F., Junk, J., & Lahlali, R. (2023). A review on UAV-based applications for plant disease detection and monitoring. *Remote Sensing*, *15*(17), 4273. https://doi.org/10.3390/rs15174273

Kushairi, A., Ong-Abdullah, M., Nambiappan, B., Hishamuddin, E., Bidin, M. N. I. Z., Ghazali, R., Subramaniam, V., Sundram, S., & Parveez, G. K. A. (2019). Oil palm economic performance in Malaysia and R&D progress in 2018. *Journal of Oil Palm Research*, *31*(2), 165–194. https://doi.org/10.21894/jopr.2019.0026

Li, W., Dong, R., Fu, H., & Yu, L. (2018). Large-scale oil palm tree detection from high-resolution satellite images using two-stage convolutional neural networks. *Remote Sensing*, *11*(1), 11. https://doi.org/10.3390/rs11010011

Liu, X., Ghazali, K. H., & Shah, A. A. (2022). Sustainable oil palm resource assessment based on an enhanced deep learning method. *Energies*, *15*(12), 4479. https://doi.org/10.3390/en15124479

Lundegårdh, H. (1943). Leaf analysis as a guide to soil fertility. *Nature*, *151*, 310–311. https://doi.org/10.1038/151310a0

Mohd Jefri, N. S., Rasib, A. W., Ahmad, A., Darwin, N., Mohd Amir, N., & Wan Yusof, W. M. H. (2023). Oil palm nutrient mapping using multispectral drone. *Journal of Advanced Geospatial Science & Technology*, *3*(2), 145–175. https://doi.org/10.11113/jagst.v3n2.73

Montoya-Sánchez, V., Camarretta, N., Ehbrecht, M., Schlund, M., Paterno, G., Seidel, D., Guerrero-Ramírez, N., Brambach, F., Hölscher, D., Kreft, H., Irawan, B., Sundawati, L., & Zemp, D. (2024). Comparing airborne and terrestrial LiDAR with ground-based inventory metrics of vegetation structural complexity in oil palm agroforests. *Ecological Indicators*, *166*, 112306. https://doi.org/10.1016/j.ecolind.2024.112306

Müller-Linow, M., Pinto-Espinosa, F., Scharr, H., & Rascher, U. (2015). The leaf angle distribution of natural plant populations: Assessing the canopy with a novel software tool. *Plant Methods*, *11*, 11. https://doi.org/10.1186/s13007-015-0052-z

Okabe, T. (2015). Biophysical optimality of the golden angle in phyllotaxis. *Scientific Reports*, *5*(1), 15358. https://doi.org/10.1038/srep15358

Ong, J. H., Ong, P., & Woon, K. L. (2022). Image-based oil palm leaves disease detection using convolutional neural network. *Journal of Information and Communication Technology*, *21*(3), 383–410. https://doi.org/10.32890/jict2022.21.3.4

Prasetyo, D. W., Kurniawan, L., Andriani, M., Putra, G. I. S., Nugraha, E. P., & Firlana. (2024). Physiological performance of oil palm inflorescences (*Elaeis guineensis* Jacq.) after drought stress on three different soil types in Central Kalimantan. *IOP Conference Series: Earth and Environmental Science*, *1308*(1), 012040. https://doi.org/10.1088/1755-1315/1308/1/012040

Prusinkiewicz, P., Zhang, T., Owens, A., Cieslak, M., & Elomaa, P. (2022). Phyllotaxis without symmetry: What can we learn from flower heads? *Journal of Experimental Botany*, *73*(11), 3319–3329. https://doi.org/10.1093/jxb/erac101

Raabe, K., Pisek, J., Sonnentag, O., & Annuk, K. (2015). Variations of leaf inclination angle distribution with height over the growing season and light exposure for eight broadleaf tree species. *Agricultural and Forest Meteorology*, *214–215*, 2–11. https://doi.org/10.1016/j.agrformet.2015.07.008

Razali, M. I. H., Hairuddin, M. A., Jahidin, A. H., Som, M. H. M., & Ali, M. S. A. M. (2022). Classification of nutrient deficiency in oil palms from leaf images using convolutional neural network. *IAES International Journal of Artificial Intelligence (IJ-AI)*, *11*(4), 1314–1322. https://doi.org/10.11591/ijai.v11.i4.pp1314-1322

Sah, P. K., Raj, A. M., & Sah, A. K. (2020). Fibonacci sequence with golden ratio and its application. *International Journal of Mathematics Trends and Technology*, *66*(3), 28–32. https://doi.org/10.14445/22315373/ijmtt-v66i3p505

Septiarini, A., Hamdani, H., Junirianto, E., Thayf, M. S. S., Triyono, G., & Henderi. (2022). Oil palm leaf disease detection on natural background using convolutional neural networks. In *2022 IEEE International Conference on Communication, Networks and Satellite (COMNETSAT)*, (pp. 388–392). IEEE https://doi.org/10.1109/COMNETSAT56033.2022.9994555

Suhartono, M. J., Setyawan, H., & Aji, W. A. (2023). Identifying plant age to determine production trend of oil palm fresh fruit bunches. *Agro Bali: Agricultural Journal*, *6*(2), 378–384. https://doi.org/10.37637/ab.v6i2.1174

Tarmizi, W. A., Muharam, F. M., & Amiruddin, A. D. (2017). Relationship between chlorophyll contents and spectral properties of frond 9 and 17 of mature oil palm. *International Conference on Big Data Applications in Agriculture (ICBAA2017)*, 214–218.

Wang, Y., Smith, R. S., & Prusinkiewicz, P. (2022). Phyllotactic patterns and leaf divergence angles in plants: A modeling perspective. *Plant Methods*, *18*, 85. https://doi.org/10.1186/s13007-022-00920-z

Wibowo, H., Sitanggang, I. S., Mushthofa, M., & Adrianto, H. A. (2022). Large-scale oil palm trees detection from high-resolution remote sensing images using deep learning. *Big Data and Cognitive Computing*, *6*(3), 89. https://doi.org/10.3390/bdcc6030089

Woittiez, L., Van Wijk, M., Slingerland, M., Van Noordwijk, M., & Giller, K. E. (2017). Yield gaps in oil palm: A quantitative review of contributing factors. *European Journal of Agronomy*, *83*, 57–77. https://doi.org/10.1016/j.eja.2016.11.002

Wong, Y. B., Gibbins, C., Azhar, B., Phan, S. S., Scholefield, P., Azmi, R., & Lechner, A. M. (2023). Smallholder oil palm plantation sustainability assessment using multi-criteria analysis and unmanned aerial vehicles. *Environmental Monitoring and Assessment*, *195*(5), 577. https://doi.org/10.1007/s10661-023-11113-z

Zachlod, N., Hudecheck, M., Sirén, C., & George, G. (2025). Sustainable palm oil certification inadvertently affects production efficiency in Malaysia. *Communications Earth & Environment*, *6*(1), 200. https://doi.org/10.1038/s43247-025-02150-2

Zhang, H., Cui, Y., Yu, L., Andino, R. E. C., Zhang, S., Cui, K., Zhao, T., & Liang, H. (2025). Single oil palm tree detection and its potential expansion in Honduras. *IEEE Transactions on Geoscience and Remote Sensing*, *63*, 4408613. https://doi.org/10.1109/TGRS.2025.3562257

Zhang, S., Li, N., Cui, Y., Dong, J., Yu, L., Ran, L., Chen, Z., Niu, J., Yan, W., Kanniah, K. D., & Xiao, X. (2025). Large-scale single tree information extraction of oil palm in Malaysia based on sub-meter visible light satellite images. *Computers and Electronics in Agriculture*, *238*, 110796. https://doi.org/10.1016/j.compag.2025.110796

Zheng, J., Fu, H., Li, W., Wu, W., Yu, L., Yuan, S., Tao, W. Y. W., Pang, T. K., & Kanniah, K. D. (2021). Growing status observation for oil palm trees using Unmanned Aerial Vehicle (UAV) images. *ISPRS Journal of Photogrammetry and Remote Sensing*, *173*, 95–121. https://doi.org/10.1016/j.isprsjprs.2021.01.008

Zou, X., Mõttus, M., Tammeorg, P., Torres, C. L., Takala, T., Pisek, J., Mäkelä, P., Stoddard, F. L., & Pellikka, P. (2014). Photographic measurement of leaf angles in field crops. *Agricultural and Forest Meteorology*, *184*, 137–146. https://doi.org/10.1016/j.agrformet.2013.09.010